In presenting the dissertation as a partial fulfillment of the requirements for an advanced degree from the Georgia Institute of Technology, I agree that the Library of the Institute shall make it available for inspection and circulation in accordance with its regulations governing materials of this type. I agree that permission to copy from, or to publish from, this dissertation may be granted by the professor under whose direction it was written, or, in his absence, by the Dean of the Graduate Division when such copying or publication is solely for scholarly purposes and does not involve potential financial gain. It is understood that any copying from, or publication of, this dissertation which involves potential financial gain will not be allowed without written permission.

3/17/65
b

THE THEORY AND PRACTICE OF DERIVATIVE CHRONOPOTENTIOMETRY

A THESIS

Presented to

The Faculty of the Graduate Division

by

William Dale Anstine

In Partial Fulfillment of

The Requirements for the Degree

Master of Science in Chemistry

Georgia Institute of Technology

June, 1969

THE THEORY AND PRACTICE OF DERIVATIVE CHRONOPOTENTIOMETRY

Approved:

Chairman

Date approved by chairman: April 28, 1969

ACKNOWLEDGMENTS

It is a pleasure to acknowledge my indebtedness to Dr. P. E. Sturrock for his guidance, inspiration and friendship. Dr. H. A. Flaschka and Dr. D. Royer also provided generous assistance during the preparation of this manuscript and in other ways as well.

TABLE OF CONTENTS

LIST OF TABLES

LIST OF ILLUSTRATIONS

CHAPTER I

INTRODUCTION

In classical chronopotentiometry a constant current is passed through the electrode system and the resulting change of the potential with time is recorded. The readout is potential vs. time (i.e., E vs. t). Sand *(1)* had derived the basic equation of chronopotentiometry as early as 1901, and thus preceded the related work of J. Heyrovsky in polarography by some 25 years. However, it was not until 1950 that Gierst and Juliard *(2)* pointed out that the dependence of the concentration of the electroactive species on the square root of the transition time had useful analytical possibilities. Since 1950 the method has been rapidly developed by many workers, and major reviews of the subject are given by Delahay *(3)* and Davis *(4)*. The theoretical treatment of conventional chronopotentiometry for both single component and multicomponent systems will be discussed in detail in Chapter II.

In order to study electrode reactions, Herman and Bard *(5)* introduced the technique of cyclic chronopotentiometry with current reversal. In this method a current is applied to the electrode, and the potential of the electrode allowed to change with time until a preset potential is reached. At the preset potential, the current is reversed and the products of the reactions formed at the electrode surface are reconverted to the original reactants. If the amount of the products at the electrode surface is changed by an additional process such as diffusion, amalgam

formation, or chemical reaction, the transition time of the next half cycle will be shortened. For example, as the potential of the electrode is made more negative metal ions are reduced at the electrode until the potential is reached at which the current is reversed. When this potential is reached, the current becomes anodic and oxidizes the metal deposited on the electrode during the previous half cycle. However, in practice the metal will diffuse away from the electrode surface and thus the anodic transition time will be less than the transition time for the cathodic half cycle.

Oscillographic Polarography with alternating current as introduced by Heyrovsky and Forejt *(6)*, and vastly extended by Kalvoda *(7)*, has many similarities to cyclic chronopotentiometry. In oscillographic polarography the electrode scans back and forth between the limiting potentials of the solution; which are, on the anodic side the oxidation of the mercury composing the electrode, and on the cathodic side reduction of the supporting electrolyte; at the frequency of the alternating current. The readout is usually dE/dt vs. E. Although most commercial instruments employ a continuous cycling technique, instruments using single-cycle polarization are desirable. Using single-cycle polarization, the sweep of the potential region is accomplished without the difficulty of reversing the current. However, in the continuous cycling apparatus, the limit of the solution is the potential at which the current is reversed. As the electrode reaches the end of the cycle, the potential is either at the anodic or cathodic limit of the solution, and thus, at the end of each cycle the potential is reducing the supporting electrolyte or oxidizing the mercury of the electrode. As the next cycle begins it is then necessary to

reoxidize the supporting electrolyte that has been formed on the previous cycle, or at the other limit, to reduce the mercury ions formed during the previous cathodic cycle. So a portion of the current is used for these processes before the potential may be made more cathodic or more anodic, and this consumption of the current before the sweep begins requires that a high direct current density be used for the electrode to complete its cycle. In addition, the absolute current density available for the faradaic process of interest is not known. The use of a programmed square wave current is also desirable, since then the current is constant during the half cycle. Both of these advantages are included in an instrument used by Kalvoda, and the results obtained on this instrument parallel closely those of cyclic chronopotentiometry.

In each of the methods discussed above there are inherent limitations. The transition times in conventional chronopotentiometry are very difficult to evaluate by graphical techniques to any degree of accuracy. When a steady state is established by continuous cycling of the current, the equations of chronopotentiometry are not applicable. The need for control of the potential limits of the working electrode is especially necessary, because a portion of the current during the next cycle is then used for decomposing of the amalgam or re-oxidizing of the supporting electrolyte.

A number of these limitations have been eliminated or minimized by a new method and a multi-purpose instrument described by Sturrock *(8)*. The method is derivative cyclic constant current voltammetry (DCCCV). In DCCCV a constant current is passed through the cell, and the current is

reversed at a preset potential as in cyclic chronopotentiometry. The potential of the working electrode then changes with time between the preset potential limits. However, instead of displaying the potential of the electrode vs. time as in classical chronopotentiometry, the voltage impulse is passed through a differentiator and the time derivative displayed as a function of either time or potential. The readout is either dE/dt vs E, or dE/dt vs t.

A discussion of the instrumentation, the theory, and the advantages and disadvantages of DCCCV will be discussed in later chapters. It is important to realize at this point that when DCCCV is limited to the first cycle or half-cycle only, then the method reduces to chronopotentiometry with a derivative readout, and is aptly called derivative chronopotentiometry.

The relationship of the transition time to the minimum of the dE/dt curves has been derived by Peters and Burden *(9)*, and is applicable only in the absence of specific adsorption effects or oxide film formation. The transition times evaluated by this derivative method have been experimentally verified by both Peters and Burden *(9)* and by Sturrock et al. *(10)*, and may be used in equations applicable to conventional chronopotentiometry.

CHAPTER II

THEORY

Chronopotentiometry is a method in which the controlled variable is the current. In this method the current is suddenly stepped from a zero value to some preset value, and the change in the potential of the electrode recorded as a function of time. The direction of the applied current determines whether the electrode process is a reduction or an oxidation. When the passage of electrons is from the electrode to the solution, the electrode is called the cathode and the process termed a reduction. Analogously, when the passage of electrons is from the solution to the electrode, the electrode is called the anode and the process termed an oxidation. The exchange of an electron across the solution-electrode interface is termed electron transfer.

When an electrode is in equilibrium with a solution, the potential of the electrode is a function of the concentrations (activities) of the electroactive species. However, by forcing a current through the cell the electrode is removed from equilibrium and the rate of electron transfer is determined by the current. If the current is maintained at a constant value, the potential of the electrode will change until a value is reached at which an electrode reaction occurs. At this potential the electroactive species is consumed and the concentration of this species at the electrode surface decreases. As the concentration of the electroactive species approaches zero, the concentration of this species at the

electrode surface is then not enough to consume the total impressed current, and as a consequence, the potential will rise to a value at which another electrode reaction supports the impressed current. The extent to which the electrode reaction occurs (in the absence of any pure chemical reactions) is determined by the slower of the two processes, the rate of the electron transfer or the rate of transport of the electroactive species to the electrode surface, or both. The process by which reactants are brought to the electrode surface or products removed from the surface is called mass transport or mass transfer, and is accomplished by three mechanisms: migration, convection, and diffusion. The simultaneous treatment of these three modes of mass transfer is very difficult. However, it is usually possible to minimize or eliminate all but one of these processes by establishing appropriate experimental conditions.

Migration involves ionic movement in the solution because of the potential gradient existing in the bulk of the solution. The current which flows due to the influence of migration is called a migration current. The migration current stems from two sources. First, charged particles move under the influence of the potential gradient existing between the two electrodes in the cell. Second, as the electrode reaction proceeds at the cathode, positive ions are removed from the solution and leave an excess of negatively charged counter ions at the electrode surface. These negative ions attract positively charged ions from the bulk of the solution, and in addition must move away from the electrode surface in order to maintain electroneutrality in the solution. The situa-

tion is analogous at the anode, but with oppositely charged species involved. The contribution of a single ion carrying a current through the solution is the product of the charge times the length of the path that it travels. The total current carried is thus the summation of all charged particles moving through the solution. So, if a high concentration of an ionic species (which is not electroactive in the potential range under consideration) is added to the solution, the current will essentially be carried completely by these inert species and the species of interest will contribute very little. Consequently, by establishment of such high concentrations of inert salt, that is, operating in the presence of a supporting electrolyte, the migration current of the species of interest can be minimized to negligible proportions. The addition of a supporting electrolyte also decreases the internal resistance of the solution, and thus decreases the IR drop across the electrodes

Convection, in the narrow sense of the term, is movement of portions of the solution due to density differences. In the broad sense, the term convection also includes agitation of the solution by mechanical stirring. The elimination of convection in chronopotentiometric measurements is essential, and thus stirring of the solution by any process is avoided. However, differences in density occur in the solution as a consequence of changes in the concentration of the electroactive species as the electrode reaction proceeds. Changes in the density of the solution may also be caused by changes in the temperature of the solution at the electrode surface. However, in practice chronopotentiometric data is not effected by convection unless the time of the electrolysis is

very long, that is, on the order of several minutes.

Diffusion occurs in solutions when there is a difference in concentration in different portions of the solution. Diffusion in a cell occurs when a concentration gradient is established between the bulk of the solution and the surface of the electrode. In chronopotentiometric experiments, the passage of current causes changes of the concentration of the electroactive species at the surface of the electrode, and establishes a concentration gradient in the solution. Thus, diffusion takes place from the bulk of the solution to the surface of the electrode, or in a few cases the reverse.

The theoretical treatment of diffusion was given by Fick *(11)* and is summarized by Murray and Reilley *(12)*. It is assumed that diffusion is linear, that is, in a single direction to a plane surface of an electrode. It is also assumed that during the electrolysis there is no change in the concentration of the electroactive species in the bulk of the solution. This is accomplished by making the cell sufficiently large; then the dimensions are said to be semi-infinite. The following derivation holds for these assumptions.

The flux at the electrode surface is defined as the number of moles, N, of the diffusing species that crosses a plane of unit area (1 cm^2) in the time dt (see Figure 1). The flux at the surface of the electrode is proportional to the concentration gradient, $\frac{\partial C}{\partial x}$, at the plane x, and is written

$$F_{(x,t)} = \frac{1}{A} \frac{dN_{(x,t)}}{dt} = D \left[\frac{\partial C_{(x,t)}}{\partial x}\right] \qquad (1)$$

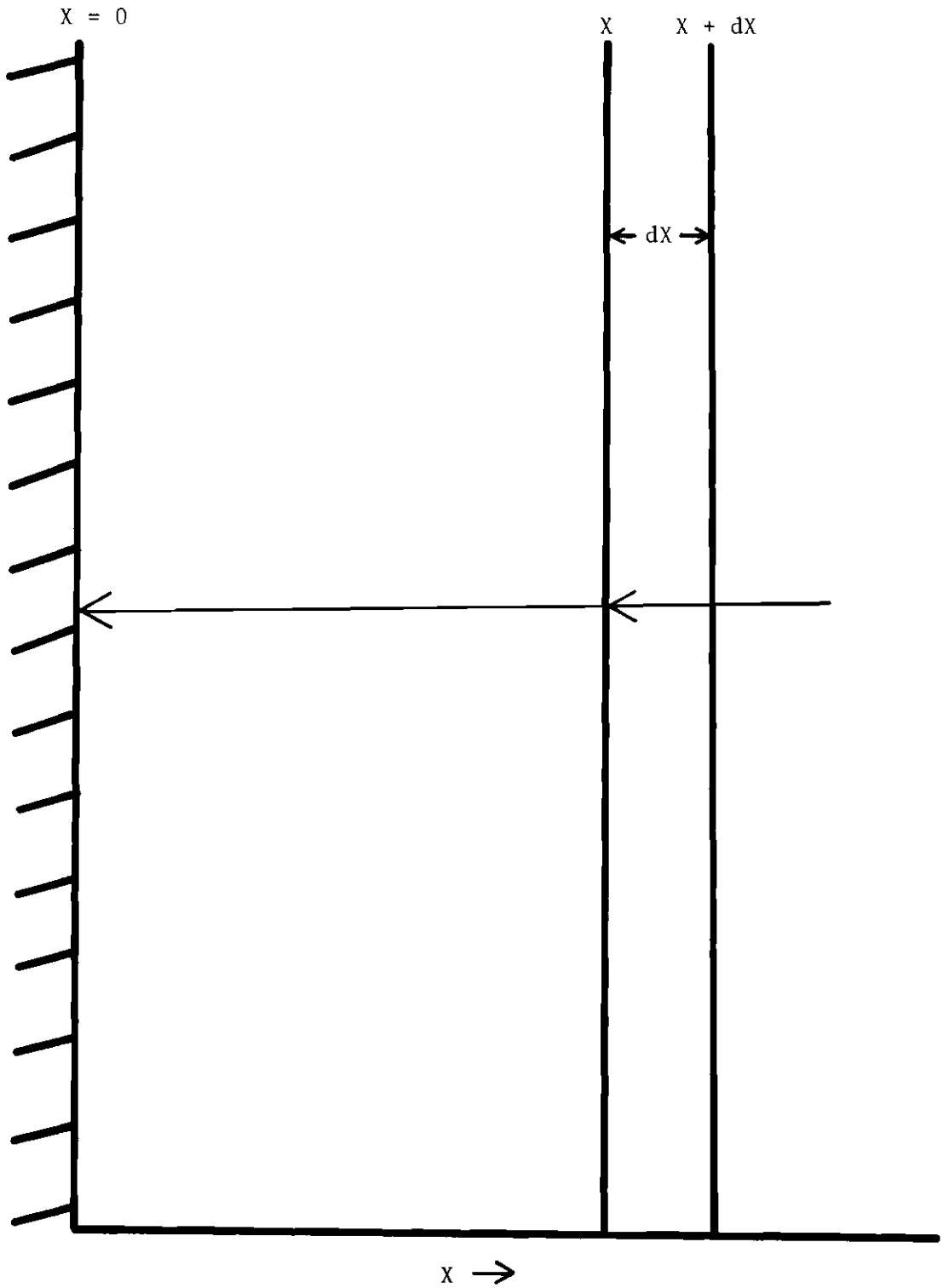

Figure 1. Linear Diffusion to a Plane Electrode.

where D is the diffusion coefficient, and x is the distance from the electrode. The term $C_{(x,t)}$ refers to the concentration of the diffusion species at the distance x from the electrode, and at a time, t, after the electrolysis has begun. This relationship is known as Fick's first law of diffusion. Equation (1) may be written to express the flux at the surface of the electrode, and yields

$$\left(\frac{\partial C_{(x,t)}}{\partial x}\right)_{x=0} = \frac{i}{nFAD} \tag{2}$$

To arrive at Fick's Second law of diffusion the flux at x + dx must be evaluated from Equation (3)

$$F_{(x + dx,t)} = D\left(\frac{\partial C_{(x,t)}}{\partial x}\right) + \frac{\partial D \left(\frac{\partial C_{(x,t)}}{\partial x}\right)}{\partial x} dx \tag{3}$$

From Equations (1) and (3) it can be deduced that the rate of change of the concentration with time between the two planes, x and x + dx, is

$$\frac{\partial C_{(x,t)}}{\partial t} = \frac{\partial [D(\partial C_{(x,t)})/\partial x]}{\partial x} \tag{4}$$

If a supporting electrolyte is used in the cell, then the diffusion coefficient may be assumed to be independent of the distance from the electrode and the time of the electrolysis. Fick's Second Law, Equation (4), may then be written in the form

$$D \frac{\partial^2 C_{(x,t)}}{\partial x^2} = \frac{\partial C_{(x,t)}}{\partial t} \tag{5}$$

The selection of appropriate boundary conditions allows us to solve this second order differential equation by the use of Laplace transforms, and to arrive at the basic relationship between current, time, and concentration under chronopotentiometric conditions.

Since the cell concentration is assumed to be homogeneous before the start of electrolysis, the initial situation is simply described by

$$C_{(x,o)} = C_{bulk} \tag{6}$$

One boundary condition is given by Equation (2) and expresses the flux at the electrode surface at any time during the electrolysis. The other boundary condition is given by

$$C_{(\infty,t)} = C_{bulk} \tag{7}$$

The solution of Equation (5) by the use of LaPlace transforms describes the concentration at any distance, x, from the electrode and any time, t, during the electrolysis, and is given in Equation (8).

$$C_{(x,t)} = C_{bulk} - \frac{2\,it^{1/2}}{nFAD^{1/2}\pi^{1/2}} \exp\left[\frac{-x^2}{4Dt}\right] + \frac{ix}{nFAD}\,\mathrm{erfc}\left[\frac{x}{2D^{1/2}t^{1/2}}\right] \tag{8}$$

The concentration of the species at the surface of the electrode, that is, at x=0, is of primary interest. For this condition Equation (8) reduces to

$$C_{(o,t)} = C_{bulk} - \frac{2\,it^{1/2}}{nFA\pi^{1/2}D^{1/2}} \tag{9}$$

The passage of current through the cell causes depletion of the electroactive species at the surface and at some time, τ, the concentration of that species becomes essentially zero. Then Equation (9) becomes

$$C_{bulk} = \frac{2\,it^{1/2}}{nFA\pi^{1/2}D^{1/2}} \tag{10}$$

Equation (10) is termed the Sand equation, and is the general equation expressing the relationship between the impressed current, the bulk concentration, and the time τ. The time τ is called the transition time and is the time elapsed between the start of the electrolysis and the depletion of the electroactive species at the electrode surface. It is the dependence of the square root of the transition time on the concentration of the electroactive species in the bulk of the solution that has useful analytical applications. The Sand equation is quite general, and holds for both reversible and irreversible processes. The actual measured transition time is independent of the rate of electron exchange and depends only on the rate of mass transport.

In the above discussion it was assumed that the total current passed through the cell was used for the electron exchange reaction (faradaic process). However, in general this is not the case because portions of the impressed current will be used for other electrode processes such as adsorption or charging of the electrical double-layer. Consequently, the Sand equation is a limiting equation that holds rigorously only at high bulk concentrations of the electroactive species, in the absence of adsorbed species.

Bard-Type Correction

The Sand equation expresses the relationship between current density, concentration, and transition time of an electroactive species, but is only rigorously valid, if the total current impressed across the cell is used for the diffusion controlled faradaic process. However, in practice portions of the total current will be used for other electrode processes such as charging of the electrical double-layer or reduction of an adsorbed species. Bard (13) has suggested a method for correcting chronopotentiometric data for charging of the double-layer, reduction of adsorbed reactant, and formation and reduction of oxides. Since the formation of oxides usually does not take place on mercury electrodes this term is deleted from the full Bard Equation giving

$$i/A = i_o = \frac{nF\pi^{1/2}D^{1/2}}{2\tau^{1/2}} C_{ox} + \frac{C_{dl}\,\Delta E}{\tau} + \frac{nF\Gamma}{\tau} \qquad (11)$$

where C_{dl} is the differential double-layer capacitance, ΔE is the potential interval, Γ is the coverage of the electrode surface, and all other symbols have their usual significance. The first term on the right side of Equation (11) is simply the Sand equation and expresses the portion of the total current which is used for the diffusion controlled faradaic process. The other terms on the right side of Equation (11) are correction terms which express the portion of the current used for charging of the double-layer $(\frac{C_{dl}\Delta E}{\tau})$, and reduction of adsorbed species $(\frac{nF\Gamma}{\tau})$.

Since no adsorbed species were encountered in the present work,

the total impressed current is distributed between the faradaic process (diffusion controlled) and the capacitive process (double-layer charging). If a chronopotentiometric constant is defined as $A = \frac{nF\pi^{1/2}D^{1/2}}{2}$, substitution of A into Equation (11) yields

$$i_o = \frac{AC}{\tau^{1/2}} + \frac{C_{dl}\Delta E}{\tau} \tag{12}$$

and further rearrangement gives

$$i_o \tau^{1/2} = AC + C_{dl}\Delta E/\tau^{1/2} \tag{13}$$

The portion of the current which is needed for double-layer charging is dependent on the bulk concentration of the electroactive species and also on the current density. At low bulk concentration of the electroactive species the double-layer process consumes a large amount of the total current. Furthermore, the use of a high current density causes the double-layer term to be more significant. The capactive process actually consumes a very small portion of the total current when the concentration of the electroactive species is high and the current density is low.

However, much of the interest in the work described here was directed towards low concentrations of inorganic metal ions, where the process of charging the double-layer consumes a significant portion of the total current. From Equation (13) it can be seen that a plot of $i_o\tau^{1/2}$ vs. concentration should be linear if the double-layer charging effect is not large, that is, if the second term in Equation (13) becomes neg-

ligible. At very short transition times, however, this approximation does not hold, and a bending of the curve toward the concentration axis will occur. Consequently, when the transition times become very short, that is, when the current density is high or the concentration is very low, the capactive process becomes significant and the correction term in Equation (13) must be included in an analysis of the data. Rearrangement of Equation (13) yields

$$i_o\tau^{1/2} - \frac{C_{dl}\Delta E}{\tau^{1/2}} = AC \qquad (14)$$

Thus, a plot of $i_o\tau^{1/2} - \frac{C_{dl}\Delta E}{\tau^{1/2}}$ vs. concentration will be linear. The plot of $i_o\tau^{1/2} - \frac{C_{dl}\Delta E}{\tau^{1/2}}$ vs. concentration takes into account the double-layer charging and effectively eliminates its significance on the empirical data.

The value of $C_{dl}\Delta E$ can be experimentally obtained from the intercept of a plot of $i_o\tau$ vs. $C\tau^{1/2}$ and the linearity of such a plot is evidence for the applicability of Equations (13) and (14).

Single Component Systems

As discussed above, the value of the transition time obtained from the Sand Equation is independent of the rate of the electron transfer, and depends only on the rate of the mass transfer to the electrode surface. Thus the length of the measured transition time affords us no information about the reversibility of the electrode reaction. However, the shape of the conventional potential-time curve is dependent on the

reversibility of the reaction proceeding at the electrode surface.

If the transfer of the electron across the solution-electrode interface is rapid (i.e., the energy barrier is small) then the rate constant for the electron transfer is large. The electrode then is essentially always in equilibrium with the electroactive species at the surface of the electrode. The potential of the working electrode is related to the concentration of the species at the electrode surface for a reversible process at 25°C by the Nernst Equation

$$E = E^{\circ} + \frac{0.0591}{n} \log \frac{[C_{ox}]}{[C_{red}]} \tag{15}$$

where E° is the standard potential of the redox couple, and C_{ox} and C_{red} are the concentrations of the oxidized and reduced species at the electrode surface respectively. However, the concentrations of the oxidized and reduced species at the electrode surface at any time $\underline{t}$ after the start of the electrolysis is given by Equation (9). Substitution of these concentrations into the Nernst Equation yields

$$E = E^{\circ} + \frac{0.0591}{n} \log \frac{\left(\tau^{1/2} - t^{1/2}\right) D_{ox}^{1/2}}{t^{1/2} D_{red}^{1/2}} \tag{16}$$

Incorporating $D_{ox}^{1/2}$ and $D_{red}^{1/2}$ into the standard potential term gives

$$E = E^{\circ\prime} + \frac{0.0591}{n} \log \frac{\tau^{1/2} - t^{1/2}}{t^{1/2}} \tag{17}$$

When the time of electrolysis, t, equals $\tau/4$ the potential of the electrode may be equated with $E^{\circ\prime}$. The potential $E^{\circ}_{1/4}$ is analogous to the half wave potential in classical polarography and is also a characteristic of the redox couple.

As the electrolysis proceeds the initial steep portion of the potential time curve is the change of the potential of the electrode until some potential is reached at which a species in the solution is electroactive. All of the current during this portion of the curve is used to charge and maintain the structure of the electrical double-layer.

When a potential is reached at which an electroactive species is reduced the potential of the electrode is determined by the concentration of the species at the electrode surface according to the Nernst Equation (only for the reversible situation). When the reactant is essentially depleted at the electrode surface, the ratio $[\frac{C_{ox}}{C_{red}}]$ is very much removed from unity, and the potential will rise rapidly until a potential is reached at which another electrode reaction supports the impressed current. The shape of the potential-time curve in this situation is determined by the concentration of the species at the electrode surface and thus when the electroactive species is depleted at the electrode surface the potential will rise very sharply.

However, as the rate constant for the electron transfer process becomes smaller the concentration of the species at the electrode surface does not solely determine the potential. The measured potential will be greater than that which corresponds to the reversible situation, and the difference is termed the overpotential. When the electrode pro-

cess has an overpotential it is irreversible in nature. The overpotential originates from a slow kinetic step in the electron transfer step. The relationship between potential and time is given for an irreversible process by

$$E = \frac{RT}{\alpha n_a F} \ln \frac{nFAC_b K_c^\circ}{i} + \frac{RT}{\alpha n_a F} \ln \frac{\tau^{1/2} - t^{1/2}}{\tau^{1/2}} \qquad (18)$$

where α is the transfer coefficient and K_c° is the rate constant at the standard potential. For an irreversible system, overpotential causes the potential vs. time curves to be distorted (see Figure 2). In the case of a reduction, the $E_{1/4}$ value will occur at more negative potentials. In order to evaluate the potential for an irreversible system the rate parameter α amd K_c° must be known.

Derivative Chronopotentiometry of Single Component Systems

The experimental methods of derivative chronopotentiometry are the same as in classical chronopotentiometry except the readout is dE/dt vs. t instead of E vs. t. This is done simply by passing the potential from the cell through a differentiating network to obtain the time derivative. A derivative chronopotentiogram for a single component system is shown in Figure 3.

The minimum in the derivative curve is related to the transition time in the classical method, and the theoretical equations have been given by Peters and Burden *(9)*.

A reduction reaction in which no C_{red} is present before the start

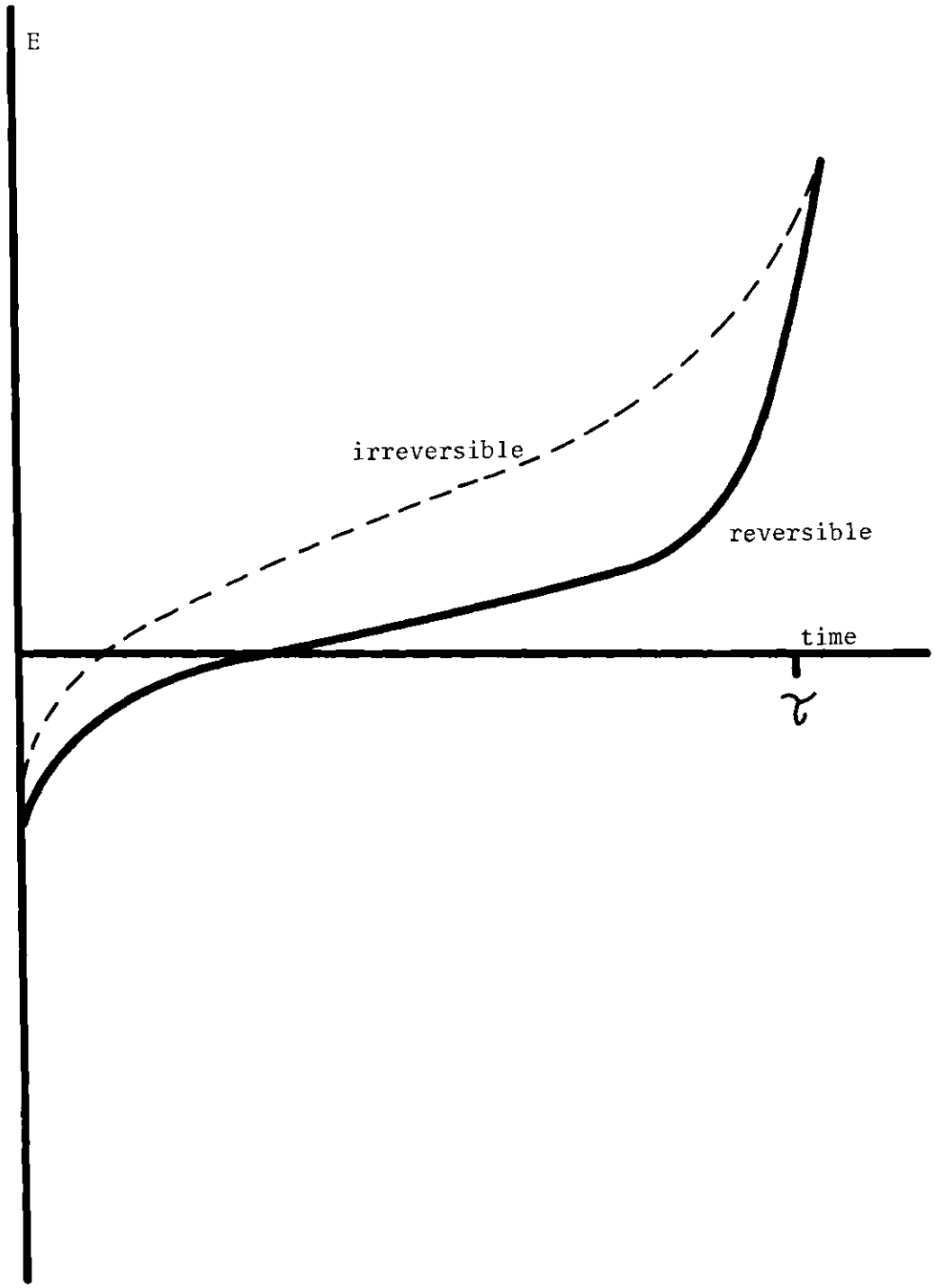

Figure 2. Classical Chronopotentiogram of a Single Component System.

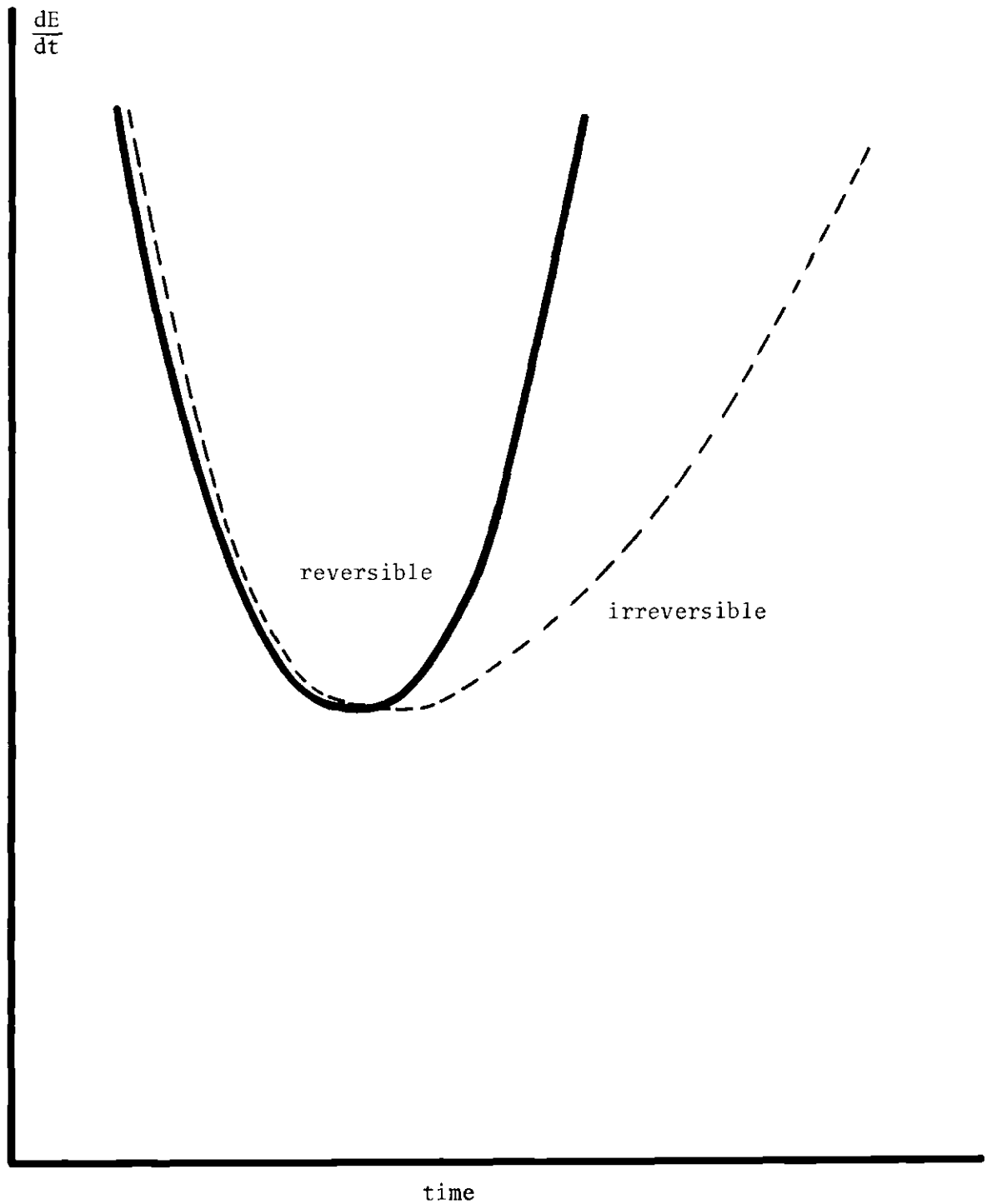

Figure 3. Derivative Chronopotentiogram of Single Component System.

of the electrolysis, and after commencement of the electrolysis both forms of the redox couple are soluble, is assumed. Peters and Burden *(9)* derived the equation for a reversible system as follows

$$\tau\left(\frac{dE}{dt}\right)_{min} = \frac{-27}{8}\ \frac{RT}{nF} \tag{19}$$

For an n=2 process at 25°C Equation (17) becomes

$$\tau\left(\frac{dE}{dt}\right)_{min} = -\ 0.04332 \tag{20}$$

The experimental verification of Equation (19) has been reported both by Peters and Burden *(9)* and Sturrock et al. *(10)*. For an irreversible system, Peters and Burden report the following relationship between $(dE/dt)_{min}$ and τ.

$$\left(\frac{dE}{dt}\right)_{min} = -\frac{2RT}{\alpha n_a F\tau} \tag{21}$$

where α is the transfer coefficient.

If τ is determined from the classical chronopotentiogram, then α may be determined from Equation (21).

The shape of the dE/dt vs. t curves also depends on the reversibility of the electrode process. As is shown in Figure 3, a reversible process has a well-defined minimum. In the irreversible case the derivative curve is displaced along the time axis (see Figure 3), and the minimum is broader. The shape of the dE/dt vs. t curves allows a distinction between reversible and irreversible electrode process.

Theoretical Extension to Multicomponent Systems

When two components are present in the solution a potential time curve appears as shown in Figure 4. The passage of current through the cell causes the potential to increase until it reaches the potential of the first redox couple. The potential then remains almost constant until the concentration of the first species is essentially zero at the surface of the electrode; then the potential rises rapidly until it reaches the deposition potential of the second couple, and levels off again until the concentration of the second species has become essentially zero at the electrode surface. However the reacting species continue to be transported to the electrode surface. Thus the overall current is a composite of the two currents related to the reactions of the two species. Consequently, the second transition time is not the same as it would be if the second species were present in the solution alone. While the second transition time is defined analogously to the transition time of the first component it does not simply relate to the concentration of the second species.

The relationship between the two transition times has been expressed mathematically by Delahay and Mamantov *(14)* as follows:

$$(\tau_1 + \tau_2)^{1/2} - (\tau_1)^{1/2} = \frac{\pi^{1/2} D_2^{1/2} n_2 FA}{\alpha i} (C_{bulk})_2 \qquad (22)$$

where the subscripts one and two refer to the first and second components in the solution respectively.

It is a purpose of this work to derive the equations which extend

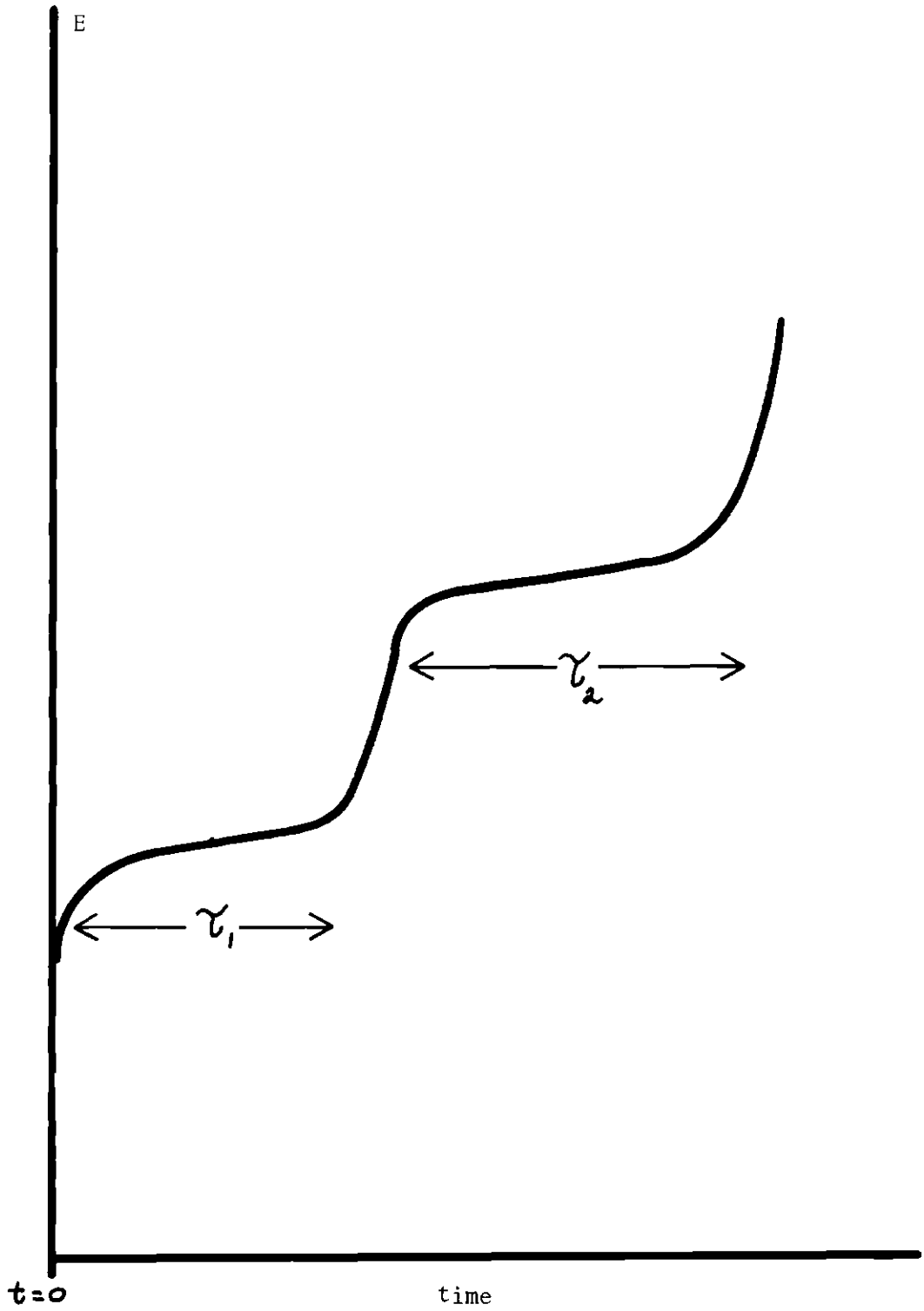

Figure 4. Potential-Time Curve of a Multi-Component System.

the theory of derivative chronopotentiometry to systems containing two or more electroactive species. The relationship between concentrations and transition times for a multi-component system is given by the Response Function Additivity Principle of Murray and Reilley *(15)*. This function is written

$$C^{*}_{o,j} = \frac{2i}{n_j F(\pi D_{o,j})^{1/2}} \left(\sum_{m=1}^{j} \tau_m \right)^{1/2} - \left(\sum_{m=1}^{j-1} \tau_m \right)^{1/2} \qquad (23)$$

where the subscript j refers to the j-th step of the chronopotentiogram. If

$$\sum_{m=1}^{j} \tau_m > t > \sum_{m=1}^{j-1} \tau_m \qquad (24)$$

then

$$D_{o,j}^{1/2}[C^{*}_{o,j} - C_{o,j}] = D_{r,j}^{1/2} C_{r,j} = \frac{2i_o}{n_j F \pi^{1/2}} x \left(t^{1/2} - \left(\sum_{m-1}^{j-1} \tau_m \right)^{1/2} \right) \qquad (25)$$

where $C_{o,j}$ and $C_{r,j}$ refer respectively to the surface concentrations of the oxidized and reduced forms of the j-th redox couple. The concentration of the reduced form in the bulk of the solution is assumed to be zero, that is, $C^{*}_{r,j} = 0$. Equation (25) is a completely general equation and holds for reversible as well as for irreversible systems. For reversible systems the E-t relationship can be obtained by substituting the concentration-time relationship into the Nernst equation.

The concentrations of the oxidized and reduced forms at the electrode surface can be obtained from Equations (23) and (25), and when these are substituted into the Nernst equation the following expression results.

$$E = E_{1/4} + \frac{RT}{n_j F} \ln \left(\frac{\left(\sum_{m=1}^{j} \tau_m \right)^{1/2} - t^{1/2}}{t^{1/2} - \left(\sum_{m=1}^{j-1} \tau_m \right)^{1/2}} \right) \qquad (26)$$

Because the Nernst equation is applicable only to reversible systems Equation (26) is valid only when the j-th redox couple is reversible.

Differentiation of Equation (26) yields

$$\frac{dE}{dt} = - \frac{RT}{2n_j F t^{1/2}} \left(\frac{1}{\left(\sum_{m=1}^{j} \tau_m \right)^{1/2} - t^{1/2}} + \frac{1}{t^{1/2} - \left(\sum_{m=1}^{j-1} \tau_m \right)^{1/2}} \right) \qquad (27)$$

In order to evaluate the minimum in the dE/dt vs $\underline{t}$ curve the derivative of Equation (27) is equated to zero. This procedure gives

$$n_j \left(\sum_{m=1}^{j-1} \tau_m \right) \left(\frac{dE}{dt} \right)_{min} = \frac{-4.5\ RT/F}{a+(a^2-a+1)^{1/2}+1} \left(\frac{1}{2a+(a^2-a+1)^{1/2}-1} + \frac{1}{a+(a^2-a+1)^{1/2}-2} \right) \qquad (28)$$

where the factor a represents

$$a = \frac{\left(\sum_{m=1}^{j} \tau_m \right)^{1/2}}{\left(\sum_{m=1}^{j-1} \tau_m \right)^{1/2}} = \frac{\sum_{m=1}^{j} n_m C^*_{o,m} D_m^{1/2}}{\sum_{m=1}^{j-1} n_m C^*_{o,m} D_m^{1/2}} = \frac{\sum_{m=1}^{j} n_m C^*_{o,m}}{\sum_{m=1}^{j-1} n_m C^*_{o,m}} \qquad (29)$$

For specific values of "a" a digital computer was programmed to print out tabular results from the solution of the right side of Equation (28).

Selected values of "a" from the computer-prepared table are shown in Table 1. The transition time for the j-th species could be determined from Equation (29) using the computer solved value of "a." The value of "a" was either calculated from Equation (29) using known concentrations or from Equation (28) by evaluation of the transition time for all previous electrode processes.

Table 1. Selected Values of "a" From Computer Prepared Table.

a	$-n_j\left(\sum_{m=1}^{j-1}\tau_m\right)\left(\frac{dE}{dt}\right)_{min}$	a	$-n_j\left(\sum_{m=1}^{j-1}\tau_m\right)\left(\frac{dE}{dt}\right)_{min}$
1.01	5.112	2.00	3.337×10^{-2}
1.02	2.544	3.00	1.216×10^{-2}
1.03	1.687	4.00	6.354×10^{-3}
1.04	1.259	5.00	3.914×10^{-3}
1.05	1.002	6.00	2.655×10^{-3}
1.06	8.312×10^{-1}	7.00	1.920×10^{-3}
1.07	7.090×10^{-1}	8.00	1.453×10^{-3}
1.08	6.173×10^{-1}	9.00	1.138×10^{-3}
1.09	5.461×10^{-1}	10.0	9.158×10^{-4}
1.10	4.891×10^{-1}	20.0	2.225×10^{-4}
1.20	2.331×10^{-1}	30.0	9.801×10^{-5}
1.30	1.483×10^{-1}	40.0	5.489×10^{-5}
1.40	1.063×10^{-1}	50.0	3.504×10^{-5}
1.50	8.141×10^{-1}	60.0	2.429×10^{-5}
1.60	6.503×10^{-1}	70.0	1.782×10^{-5}
1.70	5.350×10^{-2}	80.0	1.363×10^{-5}
1.80	4.499×10^{-2}	90.0	1.076×10^{-5}
1.90	3.849×10^{-2}	100.0	8.714×10^{-6}

CHAPTER III

INSTRUMENTATION

The instrument used for the present work was designed and built locally for the study of derivative cyclic constant current voltammetry. In this method the current is cycled through the cell and the potential vs. time curves as well as the dE/dt curves can be recorded. In addition to the derivative technique, classical chronopotentiometric curves can be obtained by displaying the potential of the working electrode as a function of time. The instrument also may be used as a multipurpose function generator for square waves and both symmetrical and unsymmetrical triangular waves. Either a two electrode or three electrode cell may be used, but it was the practice in this work to use a three electrode cell to minimize the effect of the IR drop. Various portions of the instrument are presented in block form in Figures 5, 6, and 7.

The polarizable electrode is a dropping mercury electrode or a hanging mercury drop electrode. A platinum wire serves as the counter electrode and a saturated calomel electrode as the reference electrode.

The power supply is a Philbrick PR-300 with a plus and minus fifteen volt output. The generation of the square wave from the output of the power supply is accomplished by a flip-flop amplifier (Figure 5, amplifier No. 1). The output of the flip-flop is clipped to a symmetrical square wave by a pair of five volt Zener diodes (D_1,D_2). The flip-flop is triggered as the output of the follower amplifier (Figure 5,

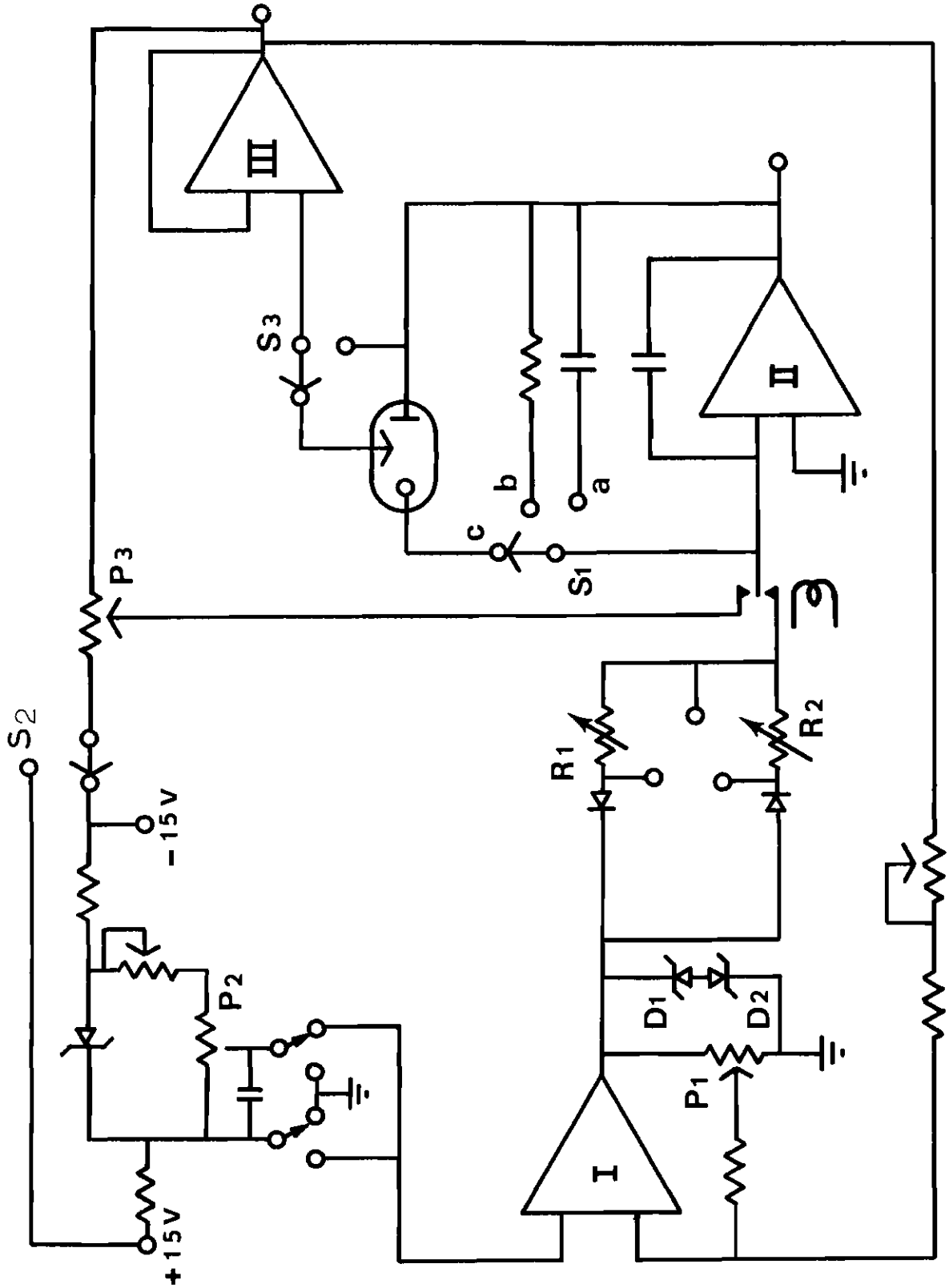

Figure 5. Current Control Circuit for Derivative Chronopotentiometer.

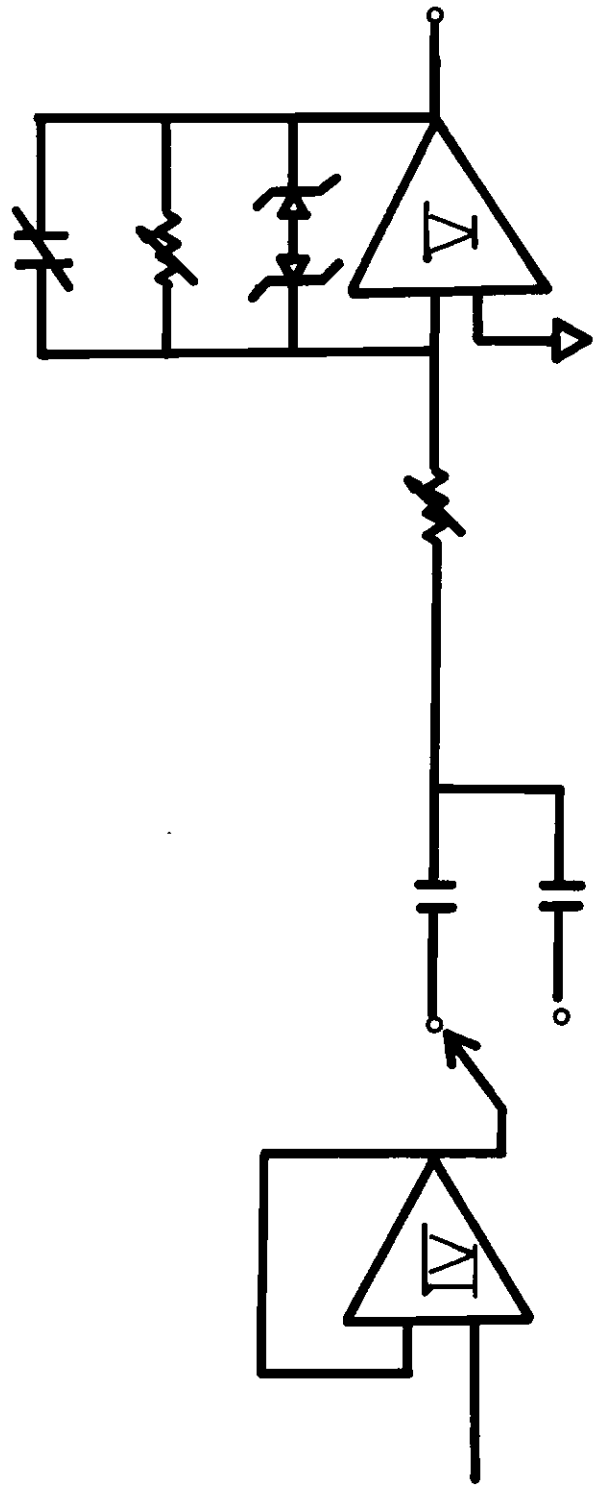

Figure 7. Differentiator Circuit for the Derivative Instrument.

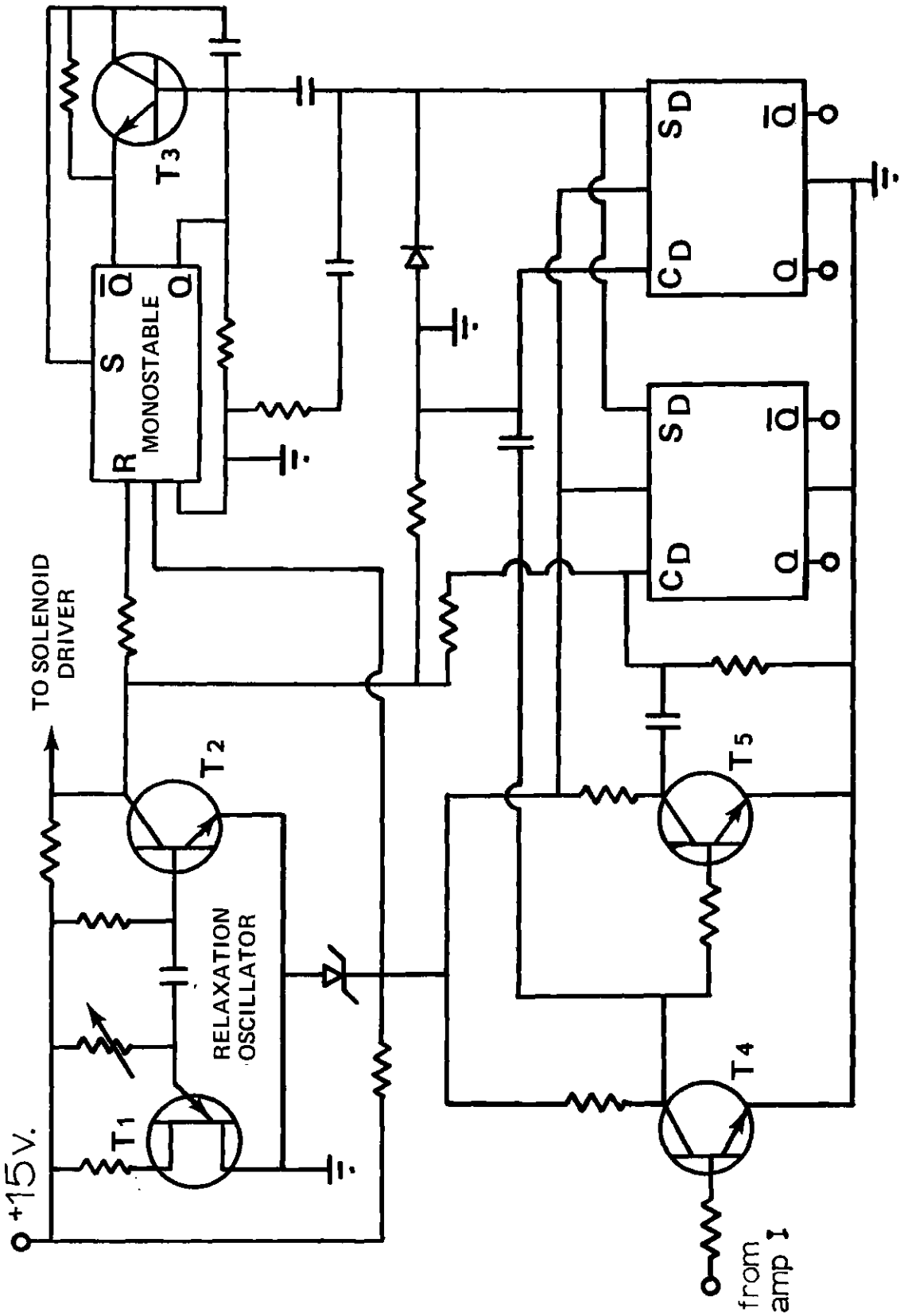

Figure 7. Timing Circuit for the Derivative Chronopotentiometer.

amplifier No. III) overcomes the positive feedback loop of amplifier I. The potential of the output of the follower thus triggers the reverse from cathodic to anodic current, or vice versa at a preset potential. The follower amplifier has a voltage gain of one and is non-inverting, so that the output potential of the follower amplifier is the same as the potential of the reference electrode compared to electrical ground. Since the test electrode is at virtual ground, the output of the follower is equal in magnitude, but opposite in polarity, to the potential of the test electrode compared to the reference electrode. For example, if the flip-flop is in the cathodic mode, the potential of the reference electrode (also the potential of the output of the follower) will become more positive until the preset potential limit is reached. Then the potential will cause the flip-flop to reverse its polarity and generate an anodic sweep. Then, the potential of the reference electrode becomes more negative. The magnitude of the potential range is set by potentiometer P_1 and the center of the potential range by potentiometer P_2.

In many applications it is necessary to vary the current passing through the cell. It is possible to vary the current used in the cathodic and anodic portions of the sweep independently of each other by the use of the two separate resistance banks, R_1 and R_2. The use of separate resistance banks has the advantage also of the possibility of generation of unsymmetrical triangular waves when a capacitor is put into the circuit in place of the cell. The resistance banks are constructed from thirteen step switches and 1% resistances which generate currents varying from 1 microampere to two milliamperes. A decade resistance box can

be used to obtain smaller changes in the current.

Amplifier No. II is the galvanostat or current control amplifier. When the switch S_1 is in the C position, the cell is in the negative feedback loop of this amplifier, and current passing through the cell is controlled by the galvanostat. The working electrode is connected directly to the summing point of the galvanostat and thus is at virtual ground. Since the sum of the currents at the summing point must be zero, the feedback current passing through the cell must equal the input current passing through the resistance banks. Thus the galvanostat controls and maintains the constant current through the cell by holding its summing point at virtual ground. When switch S_1 is in the "a" position a 0.1 microfarad capacitor is in the negative feedback loop, and the galvanostat serves as a current integrator and generates a triangular voltage wave from the square wave output of amplifier I.

The follower amplifier is the No. III amplifier, and its output voltage is effectively the voltage of the reference electrode or the counter electrode as selected by switch S_3. Amplifier No. IV (Figure 6) is am impedance matching device which is used in this function as a current booster amplifier since amplifier III cannot supply enough current to drive amplifier V and its associated circuitry.

Amplifier No. V is the differentiator which takes the first derivative of the voltage impulse with respect to time. Thirteen different combinations of a resistor and capacitor are ganged together on a thirteen position switch which thus allows thirteen positions for differentiator sensitivity. An oscilloscope display of the output of the differentiator against time yields the dE/dt vs. t curves.

It is possible to apply a prebias potential to the test electrode prior to the application of the current pulse by adjustment of switches S_2 and potentiometer P_3. The potential of the prebias can be either anodic or cathodic in direction and has a variable magnitude up to plus or minus 1.4 volts. The potential of the prebias is released by either a mercury relay or by a diode gate (not shown) when the sweep is started. The mercury relay has slower switching time than does the diode gate, but the diode gate has a small current offset. In routine work neither the slower switching time of the mercury relay or the small current offset of the diode gate caused any problems.

Figure No. 7 is the timing circuit which is used to synchronize the application of the current sweep with a desired drop size. The duty cycle is controlled by a relaxation oscillator which determines the frequency at which the drop will be detached. Thus by changing the frequency of the relaxation oscillator it was possible to vary the drop size over eleven different values. The delay cycle is a monostable oscillator which is used to delay the application of the current pulse until the desired time in the drop life. By adjustment of the delay cycle it is possible to make small changes in the effective current density. This monostable sets the two binaries to their on positions. Transitor T_3 is for fast recovery of the monostable circuit.

When the flip-flop (amplifier I) changes output polarity, transistors T_4 and T_5 are switched. Each time they are switched, one of them produces a positive going spike which will reset one of the binaries to the off position. When the binary which controls the relay or diode gate is reset, the constant current source (amplifier I) is disconnected from the galvanostat and the prebias connected, thus completing one cycle.

CHAPTER IV

EXPERIMENTAL

The instrumentation for derivative chronopotentiometry was discussed at length in Chapter III. The dE/dt vs. $\underline{t}$ curves were displayed on a Tektronic 561A oscilloscope using 3A72 dual-trace vertical amplifiers and a 3B4 time-base unit. When a permanent record was desired, the trace was photographed with a Tektronic C-12 camera using Polaroid 3000 film.

A three electrode system was used throughout the study. The experiments were performed on both hanging mercury drops and on dropping mercury electrodes. The latter was equipped with a solenoid drop detacher which was used to synchronize the fall of the drop with the application of the current pulse. A platinum wire counter electrode was used for all experiments. The reference electrode was usually a Beckman 39170 fiber-junction saturated calomel. However, in some experiments a larger locally made calomel electrode was used to reduce the noise level. The cell was a spoutless Berzelius beaker equipped with a drilled rubber stopper. The solutions were outgassed with a nitrogen bubbler of conventional design.

Since a dual-trace vertical amplifier was used, it was possible to display the conventional curve and its derivative simultaneously. With the dual-trace amplifier operated in the alternate mode, it was possible to obtain the two curves on alternate drops. It was the common

practice to photograph the curves by exposure to ten successive traces without altering the conditions. Often the traces were reproducible to such a degree that five traces photographed on each mode appeared as only one trace of each type.

It was usually the case that the relationship between the measured transition times and the change in concentration of one of the components was studied. In a two component system, the concentration of one component was held constant while that of the second was varied. Two stock solutions were usually prepared for each "concentration study." For example, in some experiments the first solution was 1.0×10^{-2} F $Pb(NO_3)_2$, 1.0 F KNO_3, and 1.0×10^{-2} F HNO_3, while a second solution contained 1.0×10^{-2} F $Pb(NO_3)_2$, 1.0 F KNO_3, 1.0×10^{-2} F HNO_3, and a known concentration of $Cd(NO_3)_2$ varying from 1.9×10^{-5} to 1.1×10^{-2} F.

A 25.0 milliliter aliquot of the first stock solution was pipetted into the cell and outgassed for fifteen minutes with nitrogen. From a ten milliliter buret, the second stock solution was added to the cell in increments of one milliliter. After each addition, the cell was outgassed for several minutes and the conventional and derivative chronopotentiograms were recorded. Since the two stock solutions contained identical amounts of lead and of supporting electrolyte, cadmium was the only cationic species which changed its concentration during the experiment. The amount of $Cd(NO_3)_2$ in the second stock solution was varied from 1.9×10^{-5} F to 1.1×10^{-2} F. For a three component system, the concentration of $Pb(NO_3)_2$ was changed to 5.0×10^{-3} F and $Cu(NO_3)_2$ in a concentration of 5.0×10^{-3} F was added to both of the stock solutions,

and the concentration of cadmium was changed over a certain concentration range. Thus in the three component system the concentrations of copper, lead, and the supporting electrolyte were held constant during the experiment.

By varying the amount of cadmium in the solution it was possible to obtain the dependence of the measured transition time on the concentration of the cadmium at a constant current density. The current densities used in these experiments varied from 2×10^{-2} to 4×10^{-2} amperes/cm^2. Such low current densities were used for the low concentrations of cadmium in order to minimize the effect of the charging of the electrical double-layer.

When a hanging mercury drop electrode (HMDE) was used, the area of the drop was known. When a dropping mercury electrode was used, it was possible to determine the area of the drop (during the short time required to make the measurement) in the following manner. The mercury height and the time-delay circuit were adjusted until the transition time which was obtained was identical to that of a hanging mercury drop of known area. In subsequent experiments it was necessary only to reset the same mercury height and delay-time to operate with the same area during the measurement. The dropping electrode was used preferentially over the hanging drop because of its convenience and better reproducibility.

Two methods were used to determine the transition times from the experimentally recorded E vs. t curves. First, the graphical method suggested by Delahay and Mamantov *(14)* as illustrated in Figure 8.

Second, the method suggested by Noonan *(16)* as presented in Figure 9. Noonan's method involves a definite potential interval over which the transition time is measured. In the latter method, a definite potential interval of 200 millivolts is taken from the intersection of lines A and B and then line C is constructed parallel to the time axis and the intersection of this line with the curve is taken as the transition time.

Determination of the transition times using the minimum in the derivative curve and Equation (20) was employed for reversible systems. In the case of a multicomponent system only the first transition time could be obtained from the derivative curve. In the three component system the first wave was irreversible in nature and thus could not be evaluated by the derivative technique.

The two graphical methods used to obtain the transition times from the conventional curves were usually compared with the transition times obtained by the derivative technique. The transition times measured by the three methods usually agreed within two per cent. The ease of evaluation of the transition time by the derivative technique made it the perferred method.

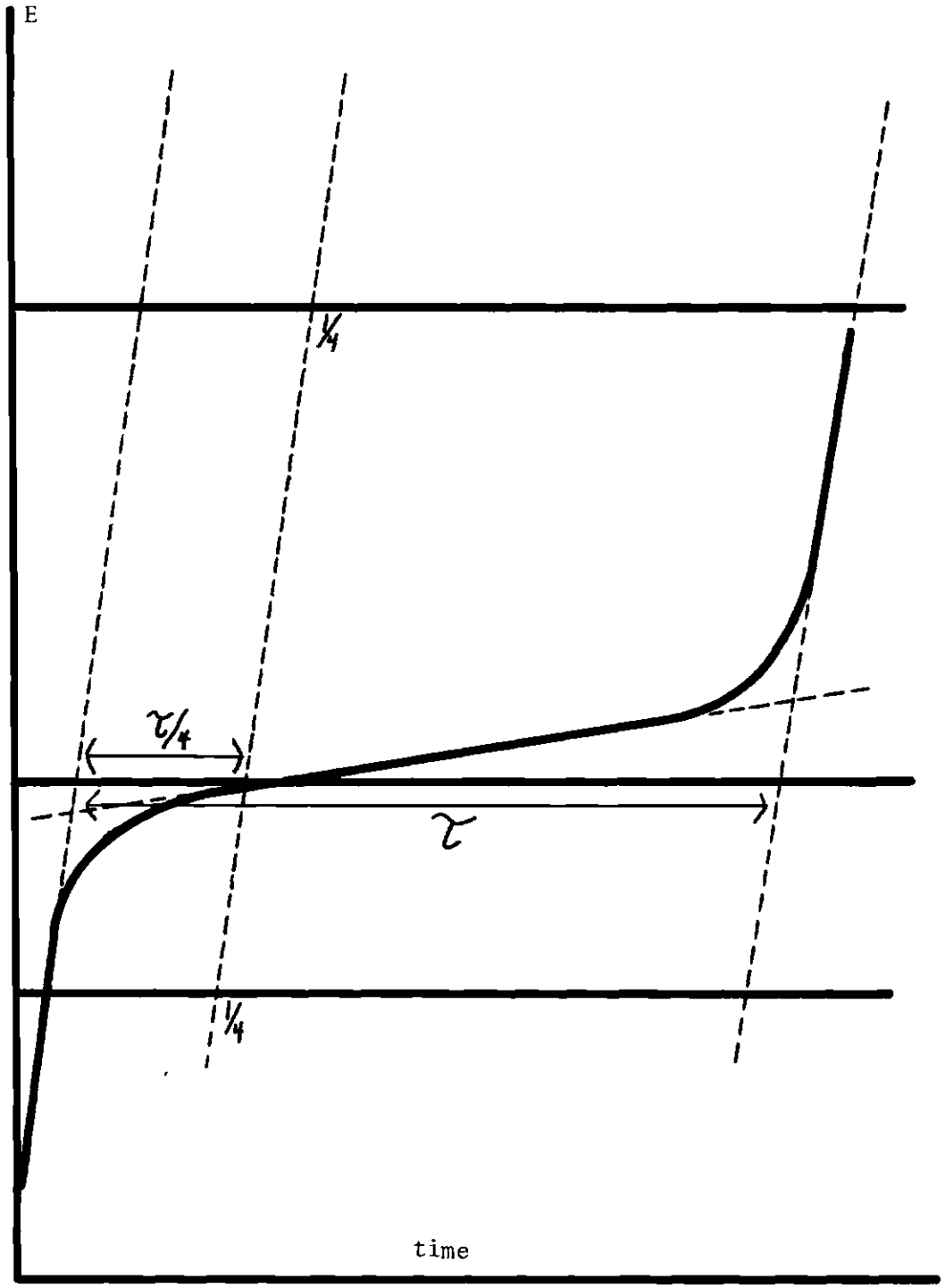

Figure 8. Graphical Method for Measuring Transition Times.

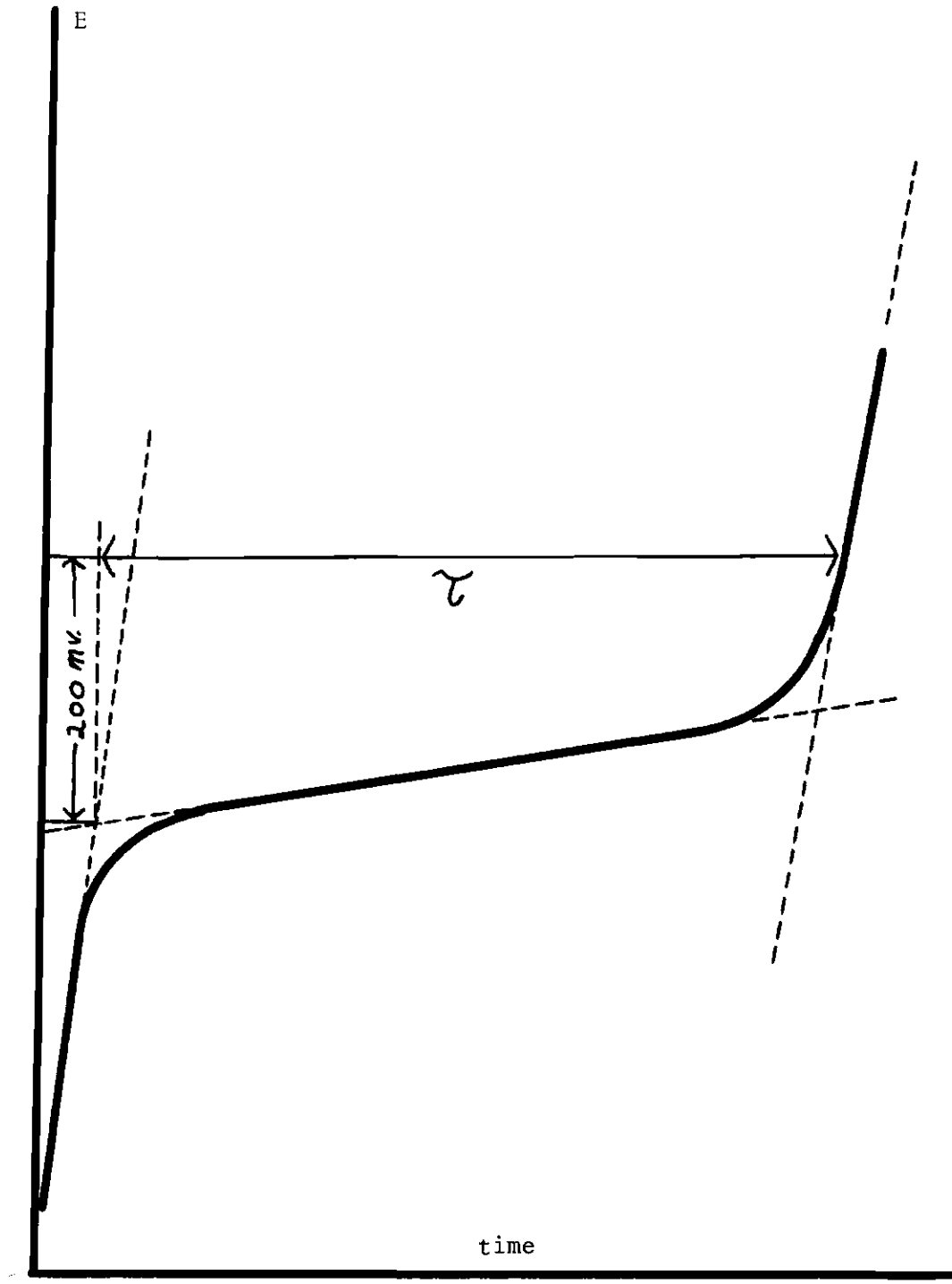

Figure 9. Noonan Method for Measuring Transition Times.

CHAPTER V

RESULTS AND DISCUSSIONS

The results of a series of experiments on a two component system (Pb-Cd) are presented in Table II. The minimum of the dE/dt curve for lead is easily read from Figure 10. Then by changing the gain of the derivative output, the dE/dt curve is magnified, and the $(dE/dt)_{min}$ for cadmium may be obtained easily from Figure 10. Since both components react reversibly, the $(dE/dt)_{min}$ for lead readily gave the lead transition time by using Equation (20) and is given at 25°C by

$$\tau_{Pb} = \frac{0.04332}{(dE/dt)_{min}} \tag{30}$$

The lead transition time was also evaluated by conventional graphical methods from potential vs. time curves (see Figure 4).

It was not possible to use an equation similar to Equation (30) for cadmium because at the potential at which cadmium is reduced the reduction of lead was occurring simultaneously. However the transition time for cadmium could be determined by the use of Equation (28) and the value of "a".

Since the transition time for lead could be obtained from the derivative curve and the values for the n_{Cd} and $(dE/dt)_{min}$ for cadmium, the numerical value of the right side of equation 28 will be experimentally evaluated. This value was then used to obtain the value of "a" from the

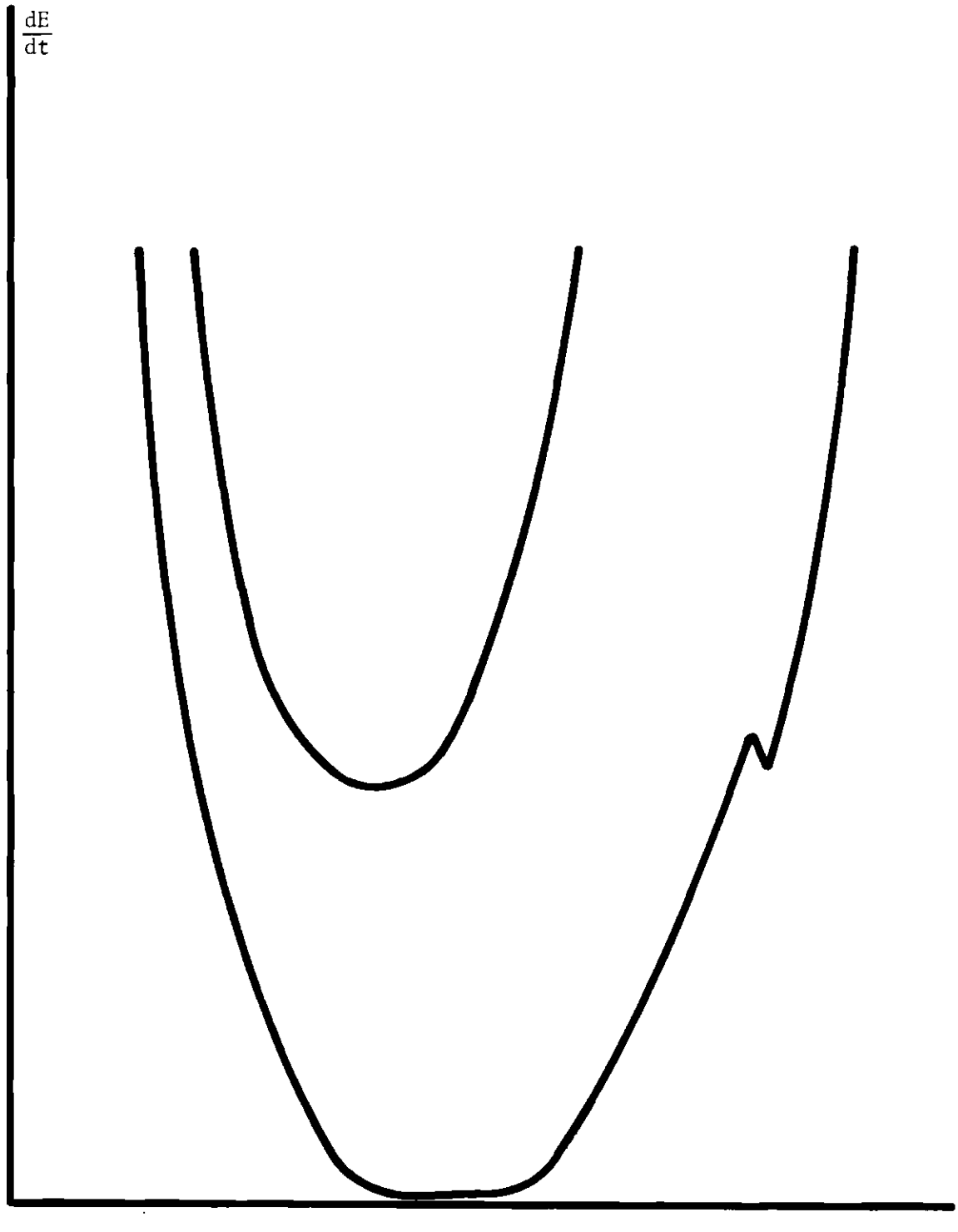

Figure 10. Typical Chronopotentiogram for Multi-Component System.

computer-prepared table. (See Table I)

The value of "a" could be arrived at in a different manner by the use of Equation (29), using the known concentrations of lead and cadmium in the calculation. The transition time for cadmium can then be evaluated from Equation (29) which explicitly written for the Pb-Cd system takes the following form:

$$\frac{(\tau_{Cd} + \tau_{Pb})^{1/2}}{\tau_{Pb}^{1/2}} = a \tag{31}$$

After multiplication by $\tau_{Pb}^{1/2}$, squaring, and rearrangement one obtains

$$\tau_{Cd} = \tau_{Pb}(a^2 - 1) \tag{32}$$

The transition times for cadmium are presented in Table II.

An interesting test of the chronopotentiometric data was the evaluation of the ratio $(D_{Cd}/D_{Pb})^{1/2}$ by an expression obtained by Equation (29) yielding

$$\left(\frac{D_{Cd}}{D_{Pb}}\right)^{1/2} = (a - 1)\frac{[Pb^{+2}]}{[Cd^{+2}]} \tag{33}$$

The results are also shown in Table II.

The value of $(D_{Cd}/D_{Pb})^{1/2}$ should remain constant when the concentration of cadmium is varied. However, one can see that as the cadmium decreases in concentration from 1.09×10^{-2} F to 3.56×10^{-4} F the value calculated for $(D_{Cd}/D_{Pb})^{1/2}$ increases slightly. This fact has been ex-

plicit in the data of other workers, and would seem to indicate a slight increase in the diffusion coefficient of cadmium as its concentration is decreased.

However, when the concentration of cadmium drops below 3.0×10^{-4} F there is a significantly more pronounced increase in the value of $(D_{Cd}/D_{Pb})^{1/2}$ as is evident in Table 2. The increase is much too large to be associated with a change in the diffusion coefficient of cadmium.

It is to be expected that when transition times are short due to low concentrations of the electrolytic species the portion of the total current used for double-layer charging will be significant. So at these low concentrations of cadmium the sudden increase in the ratio $(D_{Cd}/D_{Pb})^{1/2}$ is due to the increase in the double-layer charging contribution.

As discussed above the transition time for cadmium can be evaluated from values of "a" determined by two different methods (Equations 28 and 29). The transition times obtained from these two values of "a" usually agree within two per cent with the highest deviations at high current densities. If the values for $(D_{Cd}/D_{Pb})^{1/2}$ at cadmium concentration below 3.0×10^{-4} F are ignored, the average value of $(D_{Cd}/D_{Pb})^{1/2}$ is 0.969 with a standard deviation of 0.023. This standard deviation is well within the range of scatter of classical chronopotentiometric data for single component systems. It should also be stressed that these calculations involve four experimental parameters (two concentrations and two derivatives).

A series of experiments were performed on three component systems (Cu-Pb-Cd) and the results are presented in Table 3. It was necessary

Table 2. Derivative Chronopotentiometric Results for Two Component System.

$[Pb^{2+}]$	$[Cd^{2+}]$	i_o, $\frac{amp}{cm^2}$	τ_1, m sec	τ_2, m sec	$\frac{D_{Cd}}{D_{Pb}}^{1/2}$
9.41×10^{-3}	1.09×10^{-2}	3.8×10^{-2}	14.6	51.6	0.971
	1.01×10^{-2}			44.9	0.945
	9.25×10^{-3}			40.1	0.948
	8.35×10^{-3}			35.5	0.956
	7.39×10^{-3}			30.4	0.961
	6.36×10^{-3}			25.0	0.958
	5.26×10^{-3}			18.8	0.944
	4.09×10^{-3}			14.0	0.952
	2.93×10^{-3}			8.90	0.925
	1.47×10^{-3}			4.43	0.942
9.95×10^{-2}	1.37×10^{-3}	2.2×10^{-2}	47.6	14.2	1.014
	1.27×10^{-3}			12.8	0.994
	1.16×10^{-3}			11.7	0.990
	1.05×10^{-3}			10.5	0.993
	9.30×10^{-4}			9.19	0.988
	8.01×10^{-4}			7.87	0.989
	6.63×10^{-4}			6.39	0.977
	5.15×10^{-4}			4.99	0.989
	3.56×10^{-4}			3.34	0.967
	2.75×10^{-4}		49.1	2.87	1.043
	2.54×10^{-4}			2.69	1.056
	2.33×10^{-4}			2.43	1.042
	2.10×10^{-4}			2.18	1.036
	1.86×10^{-4}			1.98	1.064
	1.85×10^{-4}		47.6	1.94	1.087
	1.60×10^{-4}		49.1	1.80	1.130
	1.33×10^{-4}			1.59	1.201
	1.03×10^{-4}			1.40	1.362
	9.42×10^{-5}		47.6	1.26	1.394
	7.12×10^{-5}		49.1	1.16	1.634
	3.70×10^{-5}			0.96	2.625
	1.89×10^{-5}			0.87	4.646

to evaluate the combined transition time due to copper and lead by conventional graphical techniques from the experimental E vs. t curves. It was not possible to evaluate the copper transition time by the derivative technique because the copper wave was of an irreversible nature. The transition time for cadmium could be determined by the general method discussed above for a two component system. The ratio $\frac{2(D_{Cd})^{1/2}}{(D_{Cd})^{1/2}+(D_{Pb})^{1/2}}$ may be calculated by rearrangement of Equation (29) and is written explicitly for the Cu-Pb-Cd system.

$$\frac{2(D_{Cd})^{1/2}}{D_{Cd}^{1/2} + D_{Pb}^{1/2}} = (a - 1) \frac{[Cu^{+2}] + [Pb^{+2}]}{[Cd^{+2}]} \qquad (34)$$

It would also be expected that as the cadmium concentration is decreased there would be an increase in the ratio $2(D_{Cd})^{1/2}/(D_{Cd}^{1/2} + D_{Pb}^{1/2})$ due to increased contribution of the double-layer charging. The data in Table 3 is not conclusive but the suggestion is that the contribution of double-layer charging at low cadmium concentration is significant.

It was possible to approximate the transition time for copper and the combined transition time for copper and lead by the derivative technique in the following manner. Since the concentrations of copper and lead were known to be equal in these experiments, "a" was calculated from Equation (29) assuming that D_{Cu} was equal to D_{Pb}. Then the dE/dt value for the lead transition was substituted into Equation (28) and the transition time for copper calculated. Finally, the transition time for copper and "a" were substituted back into Equation (29) and the combined transi-

Table 3. Derivative Chronopotentiometric Results for Three Component System.

$[Cd^{2+}]$	$\frac{2(D_{Cd})^{1/2}}{(D_{Cu})^{1/2}+(D_{Pb})^{1/2}}$	τ_3, milliseconds
1.37×10^{-3}	0.988	15.2
1.27×10^{-3}	0.933	13.2
1.16×10^{-3}	0.948	12.0
1.05×10^{-3}	0.930	10.8
9.30×10^{-4}	0.925	9.45
8.01×10^{-4}	0.929	8.13
6.63×10^{-4}	0.904	6.50
5.15×10^{-4}	0.899	4.99
3.56×10^{-4}	0.894	3.40
1.85×10^{-4}	0.955	1.88
9.42×10^{-5}	1.206	1.20

$[Cu^{2+}] = 5.00 \times 10^{-3}$ M, $[Pb^{2+}] = 4.98 \times 10^{-3}$ M, $\tau_1 = 13.1$ m sec, $\tau_2 = 39.4$ m sec, $i_o = 2.1 \times 10^{-2}$ amps/cm^2

tion time for copper and lead waves was calculated. As an example of this procedure the calculation of the copper transition time yielded a value of 13.25 milliseconds and the combined lead and copper transition time was 53.0 milliseconds. When the values were obtained from the conventional E vs. t curves the values were 13.1 and 52.5 milliseconds respectively. The agreement between the derivative method and the conventional methods is excellent in spite of the gross assumption.

Application to Analysis

For a single component system a Bard-type correction discussed in Chapter II for double-layer charging and reduction of an adsorbed monolayer leads to very good results. This correction requires a knowledge of the separation between the faradaic and capactive portions of the total current. For a multicomponent system, however, the relationship between these two is not known. The faradaic component in a multicomponent system is not only due to the jth component, but a portion of the current is used to reduce simultaneously the j-1 electroactive species which diffuse to the electrode surface. Thus the longer the transition time for the jth component, the larger will be the contribution of the j-1 preceeding electrode reactions. Consequently, in order to describe a Bard-type correction for a multicomponent system it would be necessary to correct not only the double-layer process, but also for the portion of the current being used for the preceeding steps. A Bard-type correction for chronopotentiometric data for multicomponent systems for this reason does not seem feasible.

The relationship between the concentration of the j-th species at

the electrode surface and the measured transition time for the preceding steps (i.e., the j-1 electrode reactions) is given by

$$C^{*}_{o,j} = \frac{2i_o(a - 1)}{n_j F(\pi D_{o,j})^{1/2}} \left(\sum_{m=1}^{j-1} \tau_m\right)^{1/2} \qquad (35)$$

Knowledge of "a" and the transition time of the preceding step allows us to determine the concentration of the jth species. However, one should realize that an absolute evaluation of this type involves a large number of experimental parameters, and consequently an analytical determination on this basis is not only tedious but also subject to many errors. Practical analysis becomes most feasible when a titration or standard addition procedure is used.

A standard addition technique seems to be especially feasible because "a" is essentially independent of dilution. Thus it is only necessary to make a series of standard additions, and record the $(dE/dt)_{min}$ for each addition. Then by the use of Equation (28) the value of the right side of this equation can be obtained as discussed above, and with this value the factor "a" may be read directly from the computer-prepared table. Then a plot of (a-1) vs. "the amount of metal ion added" should yield a straight line.

Since the horizontal axis represents the amount of Cd(II) added, extrapolation to (a-1) = 0 yields a zero intercept if no Cd(II) is initially present. If however, Cd(II) was initially present in the solution then the extrapolation yields a negative intercept. A plot of (a-1) vs amount of Cd(II) added is shown in Figure 11. For this example it can

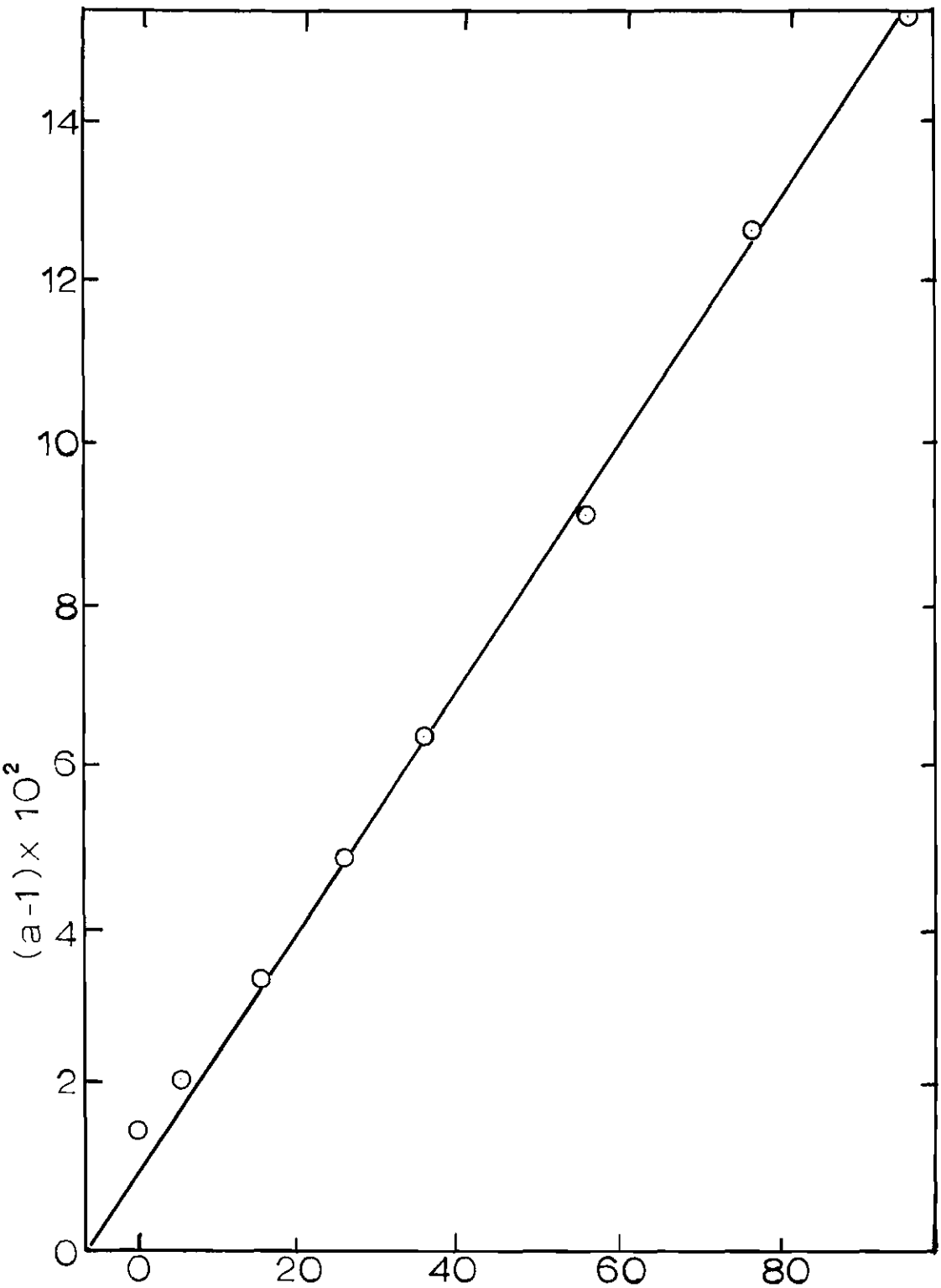

Figure 11. micromoles of Cd(II) added.

be easily read from the plot that the original Cd(II) concentration was 5.3 micromoles (in 590 micromoles of Pb(II)). The amount of Pb(II) in the solution may be determined approximately from the slope of the calibration line in Figure 11. The slope is given by

$$\text{slope} = \frac{(D_{Cd}/D_{Pb})^{1/2}}{\text{micromoles of Pb}} \tag{36}$$

At low concentration of cadmium a curvatuve in Figure 11 is noticeable. Thus it is necessary to make additions to higher concentrations where the plot is linear, and then to back extrapolate to the (a-1) axis to obtain the Cd(II) originally present.

LITERATURE CITED*

1. H. J. S. Sand, Phil. Mag., 1, 45 (1901).

2. L. Gierst and A. Juliard, Proc. Intern. Comm. Electrochem. Thermodynam. and Kinet., 2nd Meeting, Milan, 1950, pp. 117, 279.

3. P. Delahay, New Instrumental Methods in Electrochemistry, Wiley (Interscience), New York, N. Y., 1954.

4. D. G. Davis, Electroanalytical Chemistry, ed., A. J. Bard, Marcel Dekker, New York, N. Y., 1966.

5. H. B. Herman and A. J. Bard, Anal. Chem., 35, 1121 (1963).

6. J. Heyrovsky and J. Forejt, Z. Physik. Chem., Leipzig, 193, 77 (1943).

7. R. Kalvoda, Techniques of Oscillographic Polarography, Elsevier, New York, 1965.

8. P. E. Sturrock, J. Electroanal. Chem., 8, 425 (1964).

9. D. G. Peters and S. L. Burden, Anal. Chem., 38, 53 (1966).

10. P. E. Sturrock, G. Privett, and A. R. Tarpley, J. of Electroanal. Chem., 14, 303 (1967).

11. A. Fick, Pogg. Ann., 94, 59 (1855).

12. R. W. Murray and C. N. Rielley, Treatise on Analytical Chemistry, ed. I. M. Kolthoff and P. J. Elving, Section 42.

13. A. J. Bard, Anal. Chem., 35, 340 (1963).

14. P. Delahay and G. Mamantov, Anal Chem., 27, 478 (1955).

15. R. W. Murray and C. N. Reilley, J. Electroanal Chem., 3, 182 (1962).

16. D. Noonan, Ph.D. dissertation, Columbia University.

*Journal title abbreviations used are listed in "Index of Periodicals," Chemical Abstracts, 1956.